Active control of the aerodynamic performance and tonal noise of axial turbomachines

L Neuhaus[1]*, **J Schulz**[2], **W Neise**[1] and **M Möser**[3]
[1]Deutsches Zentrum für Luft- und Raumfahrt, Institut für Antriebstechnik, Abt. Turbulenzforschung, Berlin, Germany
[2]Herman-Föttinger-Institut, Technische Universität Berlin, Berlin, Germany
[3]Institut für Technische Akustik, Technische Universität Berlin, Berlin, Germany

Abstract: Two projects on axial fans are presented in this paper. The first aims at improving the aerodynamic performance and reducing the tip clearance noise caused by the rotating instability. This is achieved by injecting air into the radial gap between the impeller blade tips and the fan casing. Steady air injection with small mass flows results in remarkable reductions in the noise level along with improved aerodynamic performance. Larger injected mass flows give significant improvements in the aerodynamic performance at the expense of an increased overall noise level. The second project uses flow control actively to reduce the blade passage frequency (BPF) level. Experimental results are presented for steady jets injected into the main flow and cylindrical rods at axial positions downstream of the impeller blades. The method is successful for higher-order mode sound fields where the BPF level is reduced by up to 20.5 dB.

Keywords: active noise control, active flow control, rotating instability, tip clearance noise, axial fan, fan noise, axial turbomachine, tonal noise components, vortex generator jets, rotor/stator interaction noise, air injection

NOTATION

a_0	speed of sound
A	cross-sectional area ($A_0 = 1\,\mathrm{m}^2$)
A_{fan}	cross-sectional area of the annulus determined by the impeller and the centre body of the fan
A_{noz}	cross-sectional area of the outlet of the nozzle
c	blade chord
c_μ	momentum coefficient $= 2\,A_{\mathrm{noz}}/A_{\mathrm{fan}}\,(v_{\mathrm{jet}}\,p_{\mathrm{dyn}})^2$
d	duct diameter
D	impeller diameter
f	frequency
L_p	pressure level
L_W	sound power level
m	azimuthal mode order
m_{in}	injected mass flow in percentage of the mass flow delivered by the fan at $\varphi = 0.3$
M_{jets}	jet mass flow
M_{fan}	fan mass flow
Ma	flow Mach number $= u/a_0$
Ma_{in}	jet exit flow Mach number $= u_{\mathrm{in}}/a_0$
n	impeller speed
Δp_{stat}	static fan pressure
Δp_{t}	total fan pressure ($\Delta p_{\mathrm{t0}} = 1\,\mathrm{Pa}$)
P_{el}	electric power input to the drive motor
P_{in}	aerodynamic power of injected air flow $= M_{\mathrm{in}} u_{\mathrm{in}}^2$
s	tip clearance
St	Strouhal number $= fD/U$
u	flow velocity
u_{in}	jet exit flow velocity calculated at ambient pressure
u_∞	mean flow in the cross-sectional area A_{fan}
U	impeller tip speed
V	number of stator vanes
Q	volume flow ($Q_0 = 1\,\mathrm{m}^3/\mathrm{s}$)
Δx	axial distance
Z	number of impeller blades
Z_{noz}	number of nozzles
α	angle of the blowing direction of the nozzles relative to the mean flow
ε	hub-to-tip ratio
ζ	non-dimensional tip clearance $= s/c$

The MS was received on 31 March 2003 and was accepted after revision for publication on 7 April 2003.

**Corresponding author: Deutsches Zentrum für Luft- und Raumfahrt, Institut für Antriebstechnik, Abt. Turbulenzforschung, Müller-Breslau-Str. 8, D-10623 Berlin, Germany.*

η_t	approximate total fan efficiency $= \Delta p_t Q/(P_{el} + P_{in})$
θ	blade stagger angle
ρ_0	air density
φ	flow coefficient $= 4Q/(\pi D^2 U)$
φ_{opt}	flow coefficient at the design point
ψ	pressure coefficient $= 2\Delta p_t\ (\rho_0\ U^2)$

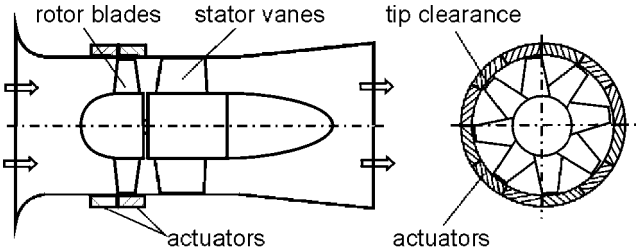

Fig. 2 Principle of the experimental set-up with actuators

1 INTRODUCTION

Axial turbomachines have a radial gap between the casing and the rotor blades. The static pressure difference between the suction and the pressure side of the impeller blades produces a secondary flow over the tip of the rotor blades (Fig. 1a). This tip clearance flow is important for the aerodynamic and acoustic performance of the machine. The pressure rise and efficiency drop and the usable range of the performance characteristic are diminished as the rotor flow is stalled at higher flow rates.

Previous work at DLR-Berlin [**1**–**4**] investigating the effects of varying tip clearances on noise and performance showed the existence of a broadband noise source for large tip–casing clearances. This source appeared in the rotor wall pressure spectrum at about half the blade passing frequency (BPF) and radiated a fluctuating tonal component into the farfield, the so-called tip clearance noise (TCN). Interpretation of the spectra and circumferential mode analyses led to the model of a rotating source mechanism, named rotating instability (RI), which moves relative to the bladerow at a fraction of the shaft speed, similarly to the cells of rotating stall [**1**, **2**]. The effect was also observed in the third stage of the low-speed research compressor at TU Dresden when the tip clearance was enlarged [**5**].

Kameier [**1**] was successful in reducing the TCN and increasing the aerodynamic performance by mounting a turbulence generator into the tip clearance gap (see also reference [**3**]) (cf. Fig. 1b). The aim of the present work is to reproduce and possibly improve the effect achieved with the turbulence generator without modifications of the tip clearance gap itself to make the method applicable also to flow machines where the tip clearance gap is changed, e.g. owing to usage of different stagger angles of the impeller blades.

The second study deals with active control of the tonal noise components of axial fans. The tonal noise of axial turbomachines is due to the periodic forces that are exerted by the flow on the rotor blades, stator vanes and the casing. As shown by Tyler and Sofrin [**6**], the interaction between the rotor and inlet flow distortions and the interaction of the wake flow off the impeller blades with the downstream stator vanes are the main causes of the blade tone spectrum of axial turbomachines.

Conventional active noise control experiments use loudspeakers to generate the secondary antiphase sound field which is superimposed destructively on the sound waves radiated from the primary source (see the papers by, for example, Burdisso *et al.* [**7**], Smith *et al.* [**8**] and Enghardt *et al.* [**9**]).

In this study, the required antiphase sound field for active noise control is produced by additional aerodynamic sound sources. This can be achieved by disturbing the flow field around the blade tips by either placing small flow obstructions such as piezoelectric actuators or small rods upstream of the impeller blade tips or by blowing air jets into the blade tip flow regime. In this way, additional periodic forces are set up on the rotor blade tips which in turn form

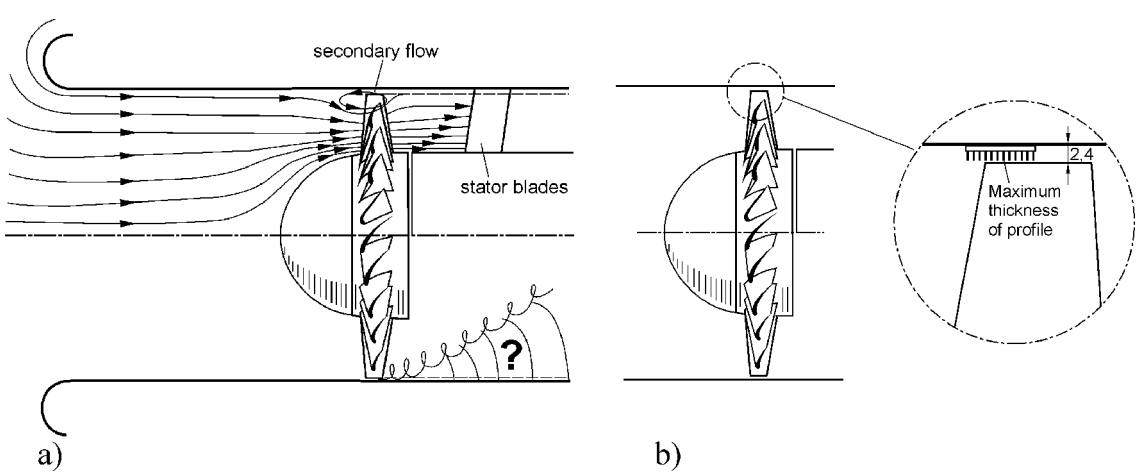

Fig. 1 Schematic view of the secondary flow driven by the pressure difference between the suction and pressure side in the tip region (left) and of the tip clearance gap with the turbulence generator inset (right)

secondary aerodynamic sound sources that are adjustable in both amplitude and phase. A principal sketch of this arrangement is depicted in Fig. 2.

2 EXPERIMENTAL FACILITIES

2.1 Test fan to improve the aerodynamic performance and suppress rotating instability and tip clearance noise

The test fan is a low-speed high-pressure axial fan with outlet guide vanes, the same as that used for earlier experiments [**1–4**]. The principal impeller dimensions are as follows: impeller diameter $D = 452.4$ mm; hub-to-tip ratio $\varepsilon = 0.62$; NACA 65 blade profile; blade number $Z = 24$; blade chord length at the tip $c = 43$ mm; maximum blade thickness 3 mm; blade stagger angle at the tip $\theta = 27°$. The design speed is $n = 3000\,\text{min}^{-1}$. The stator row comprises $V = 17$ unprofiled vanes. The axial distance between rotor and stator at the outer circumference is $\Delta x/c = 1.3$. The tip clearance can be varied by exchange of casing segments while the impeller diameter remains constant. Four casing segments are available to give the following tip clearances: $s = 0.3$, 0.6, 1.2 and 2.4 mm (normalized tip clearance $\zeta = s/c = 0.7$, 1.4, 2.8 and 5.6 per cent). All experiments reported here were made with the tip clearance of $\zeta = 5.6$ per cent.

Figure 3 shows the experimental set-up with its major dimensions. On the inlet side is a short duct section with a bellmouth nozzle. The outlet duct is anechoically terminated.

In the outlet duct a 0.5 in microphone equipped with a turbulence screen is mounted in a rotatable duct section to measure the circumferentially averaged sound pressure level at a specified radial distance from the duct axis. To measure the unsteady blade pressure, a miniature pressure sensor is mounted on the suction side of one impeller blade at 36 per cent of the chord length without changing the original outer blade contour. The radial distance from the blade tip is 7 per cent of the chord length.

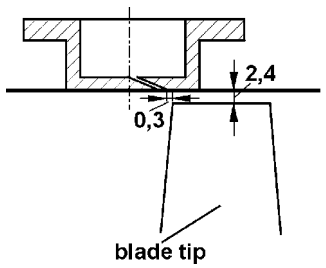

Fig. 4 Schematic view of a slit nozzle

To control the flow conditions in the tip clearance gap, air is injected into the gap through up to 24 slit nozzles mounted flush with the inner casing wall, as shown in Fig. 4. The axial position of the slit of the nozzles is 0.3 mm upstream of the impeller blades. The nozzles can be placed at up to $Z_{noz} = 24$ uniformly distributed circumferential positions. The angle between the jet axis and the interior casing wall is 15°. The slit nozzles are pivoted in the casing wall so that the angle between the main flow direction and the jets can be varied within 360°. The airflow of the injection is controlled by electronic proportional directional valves with a usable frequency range up to 200 Hz.

2.2 Test fan for active control of the tonal noise

The experiments are performed with a low-speed high-pressure axial fan with outlet guide vanes in a ducted inlet/ducted outlet configuration with anechoic terminations. A schematic presentation of the experimental set-up along with its major dimensions is shown in Fig. 5. The principal dimensions of the fan with NACA blade profiles are given in Table 1. Two different impellers are used for this study: one with $Z = 16$ and the other with $Z = 18$ blades. The volume flow rate of the fan is determined via the static pressure Δp_{stat} in the bellmouth nozzle of the inlet duct. Pressure taps in the inlet and outlet ducts are used to measure the fan pressure rise. On both fan sides, 16 wall flush mounted 0.25 in microphones, equally spaced circumferentially, are

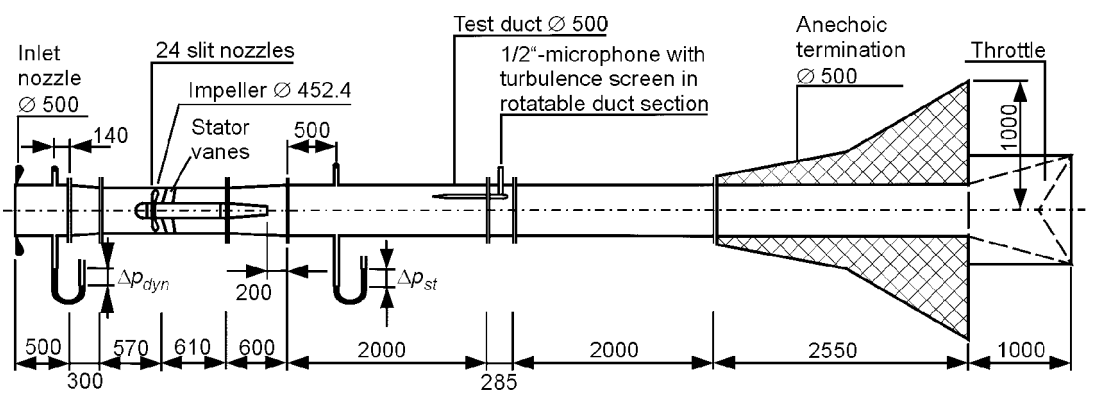

Fig. 3 Experimental set-up (dimensions in mm)

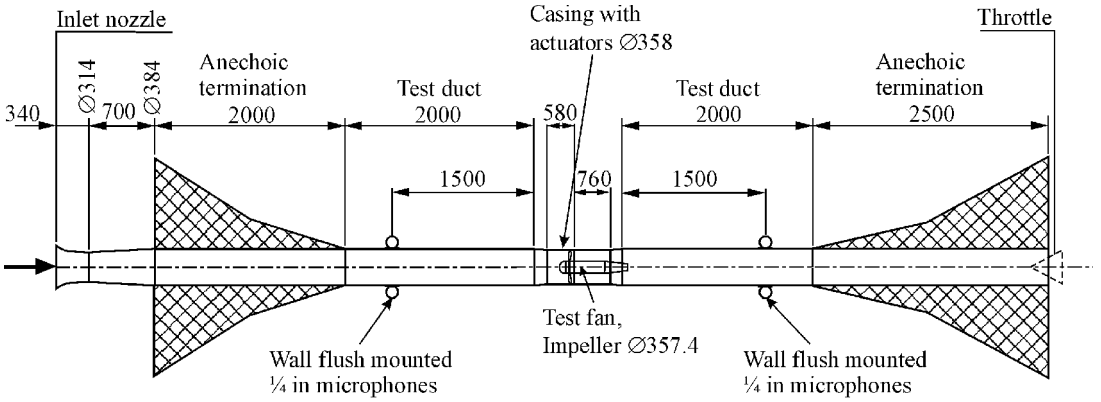

Fig. 5 Experimental set-up for the active noise control (dimensions in mm)

Table 1 Impeller dimensions

Impeller diameter	$D = 357.4\,\text{mm}$
Number of impeller blades	$Z = 16$ and 18
Blade chord length at tip	$c = 53.6\,\text{mm}$
Hub-to-tip ratio	$\varepsilon = 0.62$
Maximum blade thickness	3 mm
Blade stagger angle at the tip	$\theta = 27°$
Tip clearance ratio	$\zeta = s/c = 0.0056$
Number of stator vanes	$V = 16$
Axial rotor/stator distance	$\Delta x/c = 0.7$

used to monitor the sound fields which can be resolved into azimuthal duct modes.

To influence the flow conditions near the blade tips, small jets of compressed air are blown into the blade tip region through nozzles. Further, short cylindrical rods downstream of the impeller are tested. The actuators are installed in the fan casing wall. For results using piezoelectrical elements, refer to work by Schulz *et al.* [**10**]. Other actuator set-ups to generate the flow distortions such as small airfoils extending from the casing wall into the fan duct and short cylindrical rods upstream or downstream of the impeller are also used but will not be discussed in this paper.

The principle of the wall flush mounted nozzles is illustrated in Fig. 6a. Both the axial and the circumferential positions of the actuators are varied. One example for tested axial position and blowing directions of the nozzles is given in Fig. 6b. Compressed air is used to drive the jet flows. Figure 6c depicts the set-up for the tests using cylindrical rods for the experiments on active noise control of the BPF of the fan.

3 IMPROVEMENT IN THE AERODYNAMIC PERFORMANCE AND SUPPRESSION OF ROTATING INSTABILITY BY USING STEADY AIR INJECTION

3.1 Experiments with $Z_{noz} = 24$ slit nozzles

The first experiments were conducted with steady air injection using $Z_{noz} = Z = 24$ nozzles which is equal to the number of impeller blades. Measurements were made at the design speed $n = 3000\,\text{min}^{-1}$ of the fan. Results for reduced impeller speed and experiments with unsteady air injection are given in references [**11**] and [**12**].

Figure 7 shows the aerodynamic and acoustic performance curves for the design speed $n = 3000\,\text{min}^{-1}$. For symbols and the definitions of the non-dimensional fan performance parameters used, see the notation. The injected

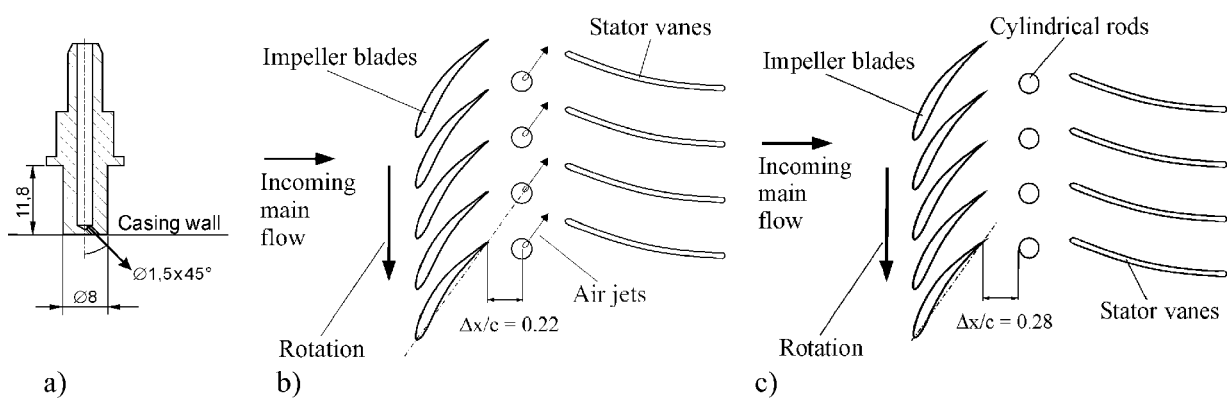

Fig. 6 Nozzles to generate the flow disturbances by air jets: (a) cross-sectional view; (b) axial position of the 16 nozzles blowing in the direction of the impeller blade chord; (c) axial position of the 16 cylindrical rods

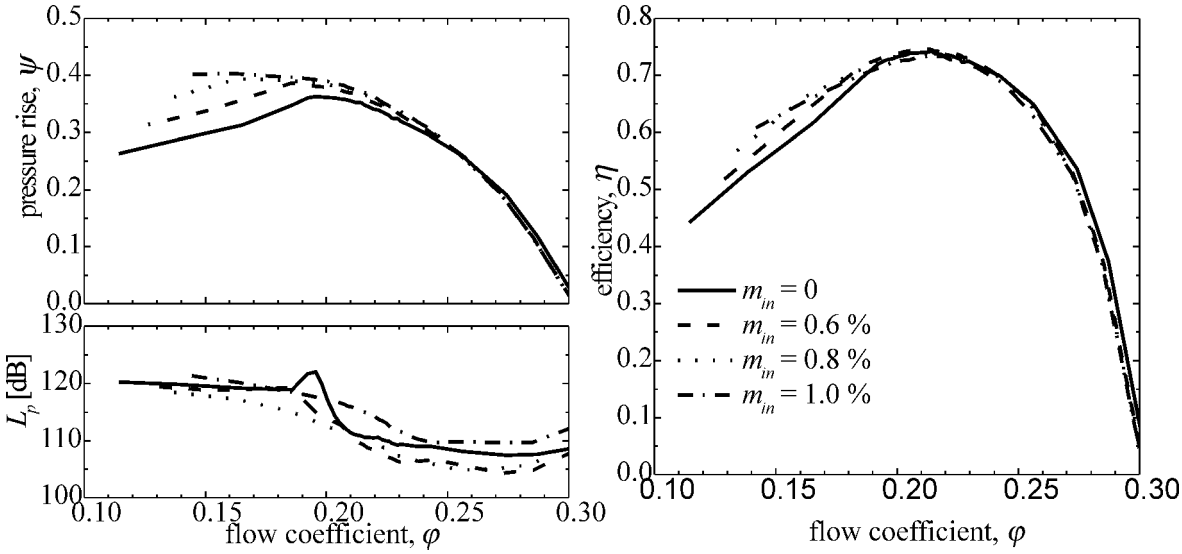

Fig. 7 Pressure coefficient, efficiency and sound pressure in the outlet duct as functions of the flow coefficient for different steady air injection mass flows; $n = 3000\,\mathrm{min}^{-1}$, $Z_{noz} = 24$, $\zeta = 5.6$ per cent

mass flow is given in percentage of the maximum mass flow delivered by the fan (i.e. at $\varphi = 0.3$). At the injected mass flow rate of $m_{in} = 0.8$ per cent, the jet flow velocity amounts to a Mach number $Ma_{in} = 0.18$. With steady air injection, pressure rise and efficiency increase at low flow rates, and the stall point is shifted towards lower flow rates. The useful range of the fan characteristic is larger with air injection than without, because the stall point is shifted. For these additional usable operation points, the pressure rise and the efficiency are then improved.

With the mass flow injection rates of 0.6 and 0.8 per cent, the optimum efficiency is increased, and with the largest rate of 1 per cent the maximum efficiency is decreased slightly. The sound pressure characteristic without air injection exhibits the occurrence of TCN at operating points near $\varphi = 0.2$. When the injected mass flow is raised to 0.8 per cent, the sound pressure level is lower over the whole range of the performance characteristics. When the injected airflow is increased further ($m_{in} = 1$ per cent), the sound pressure level becomes higher than without air injection, except for those operating points where TCN exists.

Figure 8 shows sound power spectra in the fan outlet duct and wall pressure spectra on the suction side of one impeller blade. When the injected airflow is lower than $m_{in} = 0.8$ per cent, RI is visible in the blade wall pressure spectrum and TCN in the sound pressure spectrum. When the injected mass flow rate is 0.8 per cent, RI and TCN disappear.

The level of the BPF is found to increase with the injected airflow, which is due to the interaction between the jets from the nozzles and the impeller blades. In spite of the increase in BPF level, the overall sound pressure level is reduced, e.g. at $m_{in} = 0.8$ per cent from 123 to 113 dB, where the BPF level increases from 101 to 109 dB. The changes in fan pressure and efficiency as a result of air injection are given in Fig. 8.

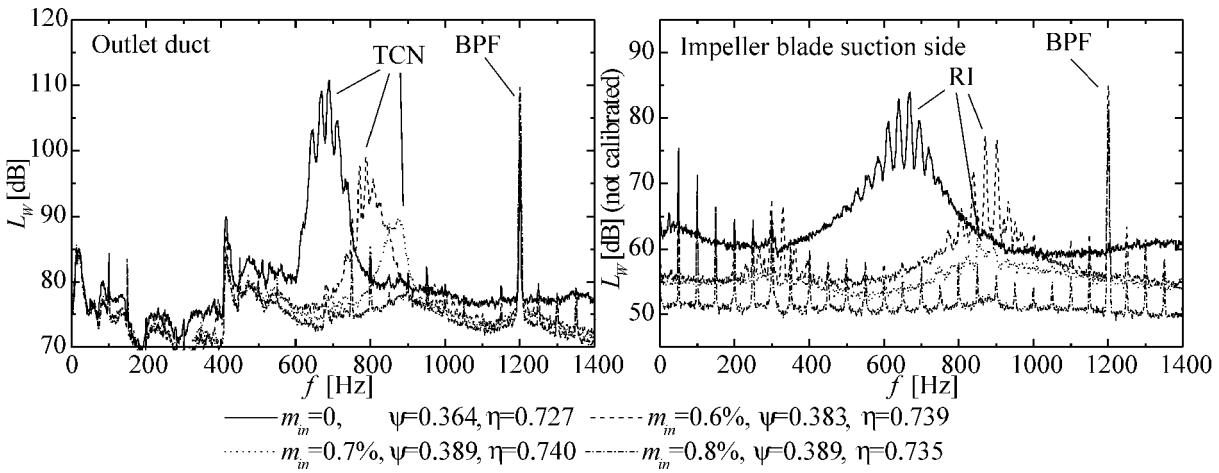

Fig. 8 Spectra of sound power in the fan outlet duct and wall pressure on the rotor blade suction side for different steady air injection rates; $n = 3000\,\mathrm{min}^{-1}$, $Z_{noz} = 24$, $\zeta = 5.6$ per cent, $\varphi = 0.2$

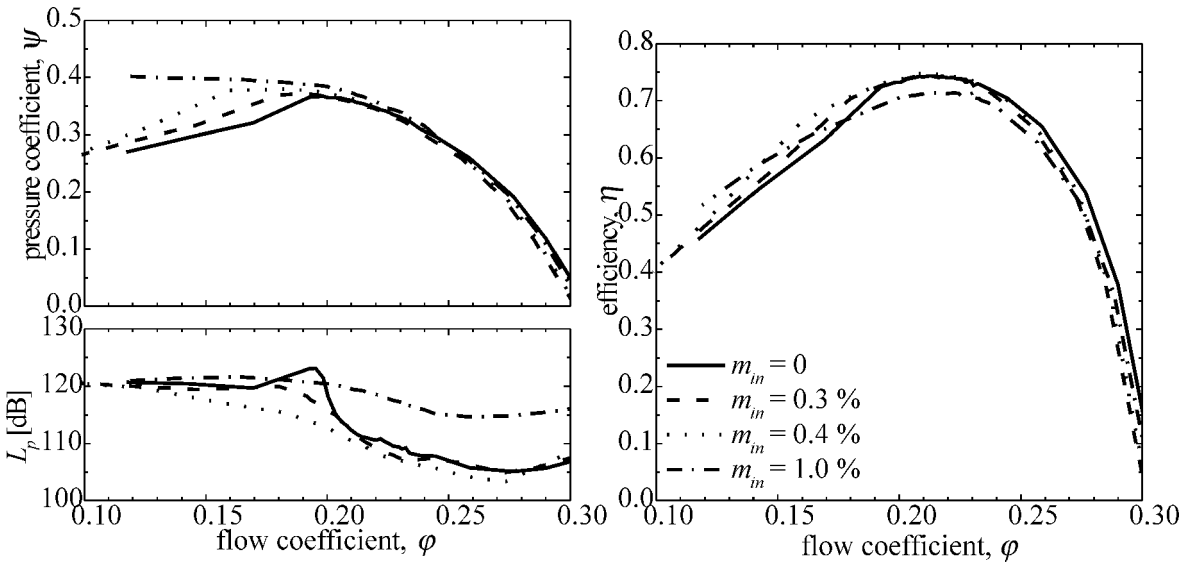

Fig. 9 Pressure coefficient, efficiency and sound pressure in the outlet duct as functions of the flow coefficient for different steady air injection mass flows; $n = 3000\ \text{min}^{-1}$, $Z_{noz} = 12$, $\zeta = 5.6$ per cent

3.2 Experiments with $Z_{noz} = 12$ slit nozzles

To demonstrate the influence of the number of injection nozzles, Fig. 9 shows the aerodynamic and acoustic fan performance curves when only $Z_{noz} = 12$ evenly distributed slit nozzles are used. As in the case with $Z_{noz} = 24$ (cf. Fig. 7), fan pressure and efficiency increase at low flow rates when steady air injection is applied. The stall point in the case $Z_{noz} = 12$ and $m_{in} = 0.4$ per cent is nearly the same as in the case $Z_{noz} = 24$ and $m_{in} = 0.8$ per cent. The optimum efficiency is improved slightly at small air injection rates and somewhat impaired at higher rates. This loss in optimum efficiency is larger for $Z_{noz} = 12$ than for $Z_{noz} = 24$. The acoustic fan performance is improved over the whole range of flow coefficients for injection rates below or equal to $m_{in} = 0.4$ per cent.

The corresponding spectra of sound power in the fan outlet duct and suction-side blade wall pressure spectra are shown in Fig. 10 for the operating point $\varphi = 0.2$. RI and TCN are completely suppressed when the injected mass flow is $m_{in} = 0.4$ per cent or higher. At $m_{in} = 0.4$ per cent, the BPF level is increased from 101 to 105 dB, nevertheless the overall level is reduced by about 10 dB down to 113 dB. Further increasing the injected airflow leads to higher BPF levels and, in turn, to smaller reductions in the overall level. In the blade wall pressure spectra a peak appears at half the BPF, which is the 'jet passing' frequency sensed by the rotating impeller blades.

Comparing the results with 12 and 24 nozzles leads to the conclusion that the injected mass flow that is needed for the complete suppression of RI and TCN is reduced by 50 per cent when only half as many nozzles are used. In both cases the velocity of the injected air is the same, $Ma_{in} = 0.18$.

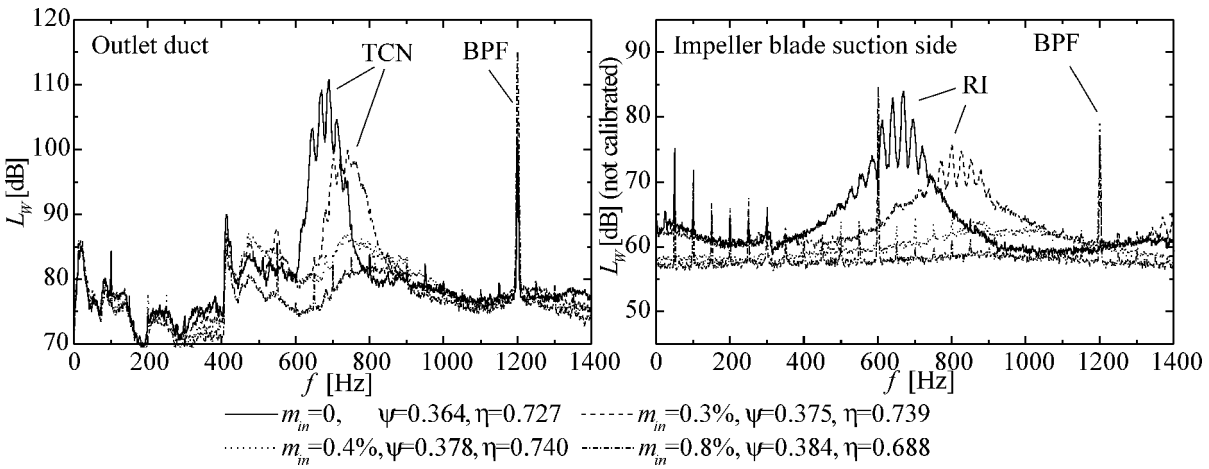

Fig. 10 Spectra of sound power in the fan outlet duct and wall pressure on the rotor blade suction side for different steady air injection rates; $n = 3000\ \text{min}^{-1}$, $Z_{noz} = 12$, $\zeta = 5.6$ per cent, $\varphi = 0.2$

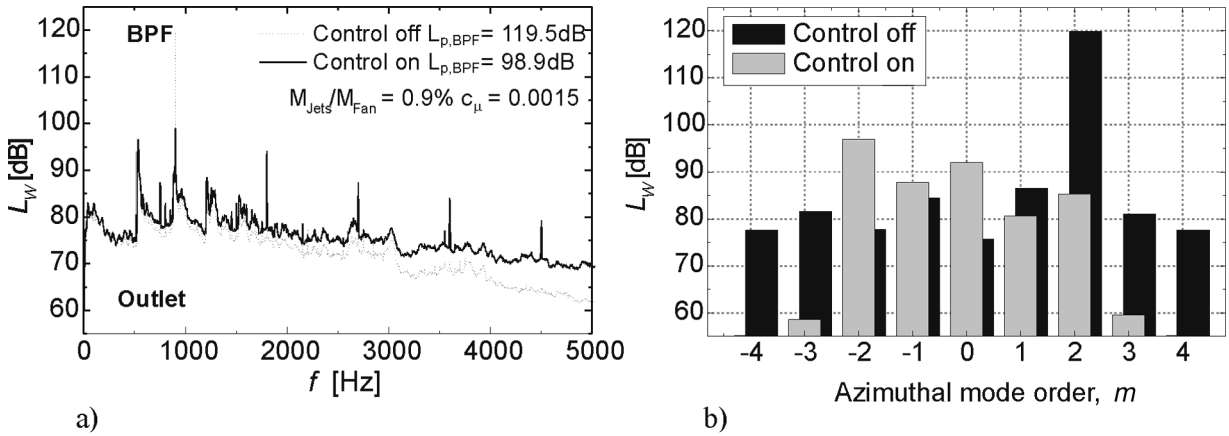

Fig. 11 (a) Sound power spectra in the outlet duct with steady air jets and (b) azimuthal mode spectra at the BPF; nozzles placed $\Delta x/c = 0.22$ downstream of the impeller blade trailing edges blowing in the direction of the blade chord; $n = 3000\,\text{min}^{-1}$, $Z = 18$, $V = 16$, $\varphi = \varphi_{\text{opt}}$

4 ACTIVE FLOW CONTROL FOR CONTROL OF HIGHER-ORDER MODE SOUND FIELD AT THE BPF

In the first phase of the experiments, 16 rotor blades and 16 stator vanes were used, and thus the sound field generated by rotor/stator interaction is dominated by the plane wave. Active noise control with both steady and unsteady blowing was tested successfully; for more details on these investigations, see references [**10**] and [**13**].

For the second phase of the study, an impeller with $Z = 18$ blades is installed while the number of stator vanes remains unchanged. This results in a dominant duct mode of azimuthal order $m = 2$ at the BPF, which is propagational in the fan duct at frequencies above 860 Hz. Only experiments with steady blowing are possible here. In the experiments, 16 nozzles, which is equal to the number of stator vanes, are used to generate the same azimuthal mode as the primary rotor/stator interaction. The axial positions of the nozzles as well as the jet directions relative to the main flow are varied. The experiments are performed at impeller speeds of 3000 and 4000 min^{-1} where the BPF is 900 and 1200 Hz respectively.

A general finding of these tests is that the method proposed is applicable to higher-order mode sound fields, which is important for the turbomachines used in practice. Figure 11a shows the circumferentially averaged sound pressure spectrum for the case of steady blowing at an axial position 12 mm ($\Delta x/c = 0.22$) downstream of the impeller in the direction of the impeller blade trailing edges. The BPF level reductions in the outlet and inlet ducts are 20.5 and 5 dB respectively. Owing to the distance between the impeller and the jets, the higher harmonics of the BPF are not increased by as much as in other experiments with a smaller axial distance, (cf. reference [**10**]). The broadband noise level is higher by a few decibels, which is due to the noise of the air injection itself.

Figure 11b shows the azimuthal mode spectrum for the BPF components at 900 Hz with and without steady blowing for the case considered in Fig. 11. As expected, the dominant azimuthal mode without control is $m = 2$. When steady blowing is applied, this mode is reduced drastically and consequently the BPF level decreases.

Experiments with this nozzle arrangement were also made at $n = 4000\,\text{min}^{-1}$. Owing to the lower mass flow ratio, and hence the lower momentum of the air jets relative to that of the main flow, the maximum possible level reduction of the BPF of 1200 Hz was only 11.5 dB.

To obtain a better understanding of the physical mechanisms involved in the interaction of the air jets and the rotor blades, flow visualization experiments were carried out with a stationary two-dimensional blade cascade using PIV measurement technique. The investigation revealed that the air injection produces vortex generator jets causing additional unsteady longitudinal structures in the flow. For the ANC experiments, this can be interpreted as the generating mechanism of the additional aeroacoustic sources with dipole characteristics. For more details on these results, see reference [**13**].

Further experiments with the impeller with $Z = 18$ blades were then performed using cylindrical rods to disturb the flow for the generation of the secondary antiphase sound field. At different impeller speeds, the axial and circumferential positions of these short cylindrical rods were varied.

Figure 12a shows the circumferentially averaged sound pressure spectrum at an impeller speed of 4000 min^{-1} (BPF = 1200 Hz) with and without short cylindrical rods extending radially $\Delta r/c = 0.37$ (30 per cent of the hub-to-tip distance) into the annular duct $\Delta x/c = 0.28$ behind the impeller blade trailing edges (refer to Fig. 6c). The BPF level reduction in the outlet duct amounts to 12.6 dB. The

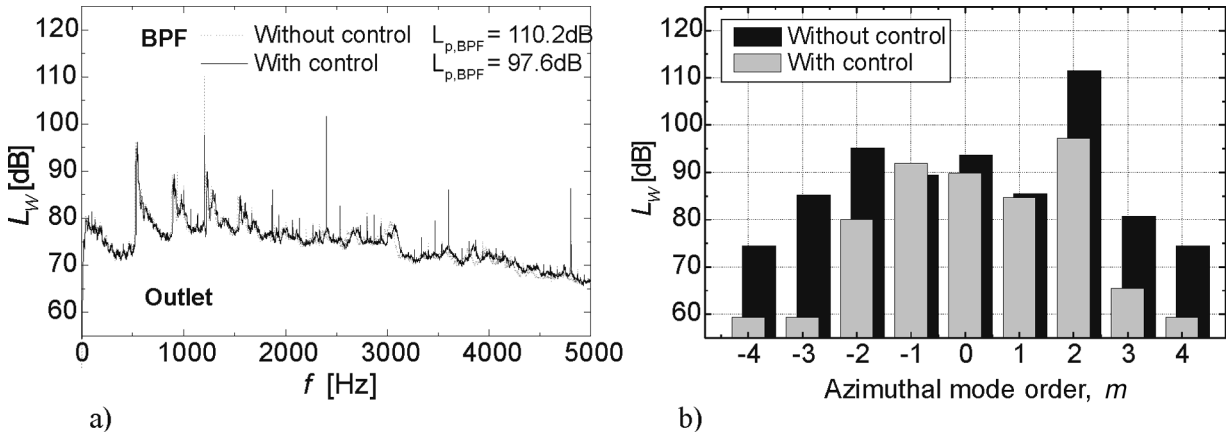

Fig. 12 (a) Sound power spectra in the outlet duct with 16 cylindrical distortions and (b) azimuthal mode spectra at the BPF; cylindrical rods placed $\Delta x/c$ downstream of the impeller blade trailing edges and extending $\Delta r/c = 0.28$ from the duct wall into the flow; $n = 4000\,\mathrm{min}^{-1}$, $Z = 18$, $V = 16$, $\varphi = \varphi_{opt}$

azimuthal mode spectra at the BPF component at 1200 Hz in Fig. 12b show the reduction in the dominant mode of azimuthal order $m = 2$. These results prove that, in general, flow distortions are suitable to generate the aeroacoustic sources needed for active noise control of the tonal components of an axial fan.

5 CONCLUSIONS

Improvements in the aerodynamic performance and suppression of the rotating instability of axial turbomachines can be obtained with steady or unsteady air injection into the tip clearance gap between the impeller blades and the fan casing. Slit nozzles mounted flush with the inner casing wall are used for the present experiments. Results for unsteady air injection are given in references [**11**] and [**12**].

With steady air injection it is possible to achieve, with small injected mass flow rates, a significant reduction in the radiated noise level together with small improvements in the aerodynamic performance, or, with high injected mass flow rates, significant improvements in the aerodynamic performance at the expense of a strong increase in the radiated noise level. Rotating blade flow instability and tip clearance noise disappear from the spectrum when steady air injection is applied. In the present experiments, the number of injection nozzles used was equal to the impeller blade number or half of it. Best results were obtained with uniform circumferential distributions [**11**]. For the fan design speed $n = 3000\,\mathrm{min}^{-1}$ the required injection velocity is $Ma_{in} = 0.18$. The necessary velocity does not scale linearly with the rotor speed or the flow velocity in the fan duct [**11**].

To obtain a better understanding of the physical mechanisms involved in the interaction of the air jets and the rotor blades, a flow investigation with a simplified stationary two-dimensional blade cascade shows that steady air injection leads to a diminished blade tip vortex and, with it, to an improved aerodynamic performance [**12**].

The tonal noise components of an axial turbomachine can be reduced using aeroacoustic sound sources for active noise control. The secondary sound field can be generated by actively controlling the flow around the impeller blade tips. Both amplitude and phase can be controlled in such a way that a destructive superposition with the primary sound field is possible. The method proposed is applicable for sound fields with higher-order modes.

The flow distortions can be achieved using different actuators. In this paper, results using steady jets of compressed air and short cylindrical rods are shown. With steady air injection, the sound pressure level at the BPF is reduced by up to 20.5 dB. An azimuthal mode analysis shows that the dominant azimuthal mode of order $m = 2$ is suppressed by more than 30 dB in this case. The reduction at the BPF using the cylindrical rods amounts to 12.6 dB.

In these experiments, too, flow investigations with a simplified stationary two-dimensional blade cascade showed that the injected air jets cause unsteady longitudinal flow structures in the blade tip region, i.e. they act as vortex generator jets, and generate additional unsteady forces on the rotor blades which in turn are the desired secondary aeroacoustic sound sources needed for controlling the primary sound waves [**13**].

ACKNOWLEDGEMENT

The investigations are supported by the German National Science Foundation as part of the 'Sonderforschungsbereich 557, Beeinflussung komplexer turbulenter Scherströmungen' conducted at the Technical University of Berlin.

REFERENCES

1 **Kameier, F.** Experimentelle Untersuchungen zur Entstehung und Minderung des Blattspitzen-Wirbellärms axialer

Strömungsmaschinen. Diss., Fortschr.-Ber. VDI series 7(243), 1994 (VDI-Verlag, Düsseldorf, Germany).

2 **Kameier, F.** and **Neise, W.** Rotating blade flow instability as a source of noise in axial turbomachines. *J. Sound and Vibr.*, 1997, **203**, 833–853.

3 **Kameier, F.** and **Neise, W.** Experimental study of tip clearance losses and noise in axial turbomachinery and their reduction. *Trans. ASME J. Turbomach.*, 1997, **119**, 460–471.

4 **März, J., Hah, Ch.** and **Neise, W.** An experimental and numerical investigation into the mechanisms of rotating instability. ASME Turbo Expo 2001, New Orleans, Louisiana, 4–7 June 2001, paper 2001-GT-0536.

5 **Müller, R.** and **Mailach, R.** Experimentelle Untersuchungen von Verdichterinstabilitäten am Niedergeschwindigkeits-verdichter. VDI Berichte 1425, Dresden, Germany, 1998, pp. 167–176.

6 **Tyler, J. M.** and **Sofrin, T. G.** Axial flow compressor noise studies. *Trans. Soc. Automot. Engrs*, 1962, **70**, 309–332.

7 **Burdisso, R. A., Fuller, C. R.** and **Smith, J. P.** Experiments on the active control of a turbofan inlet noise using compact, lightweight inlet control and error transducers. 1st CEAS/AIAA Aeroacoustics Conference, Munich, Germany, 1995, CEAS/AIAA-95-28.

8 **Smith, J. P., Burdisso, R. A.** and **Fuller, C. R.** Experiments on the active control of inlet noise from a turbofan jet engine using multiple circumferential control arrays. 2nd AIAA/CEAS Aeroacoustics Conference, State College, Pennsylvania, 6–8 May 1996, AIAA/CEAS-96-1792.

9 **Enghardt, L., Tapken, U., Neise, W. Schimming, P., Maier, R.** and **Zillmann, J.** Active control of fan from high-bypass ratio aeroengines; experimental results. 7th International Congress on *Sound and Vibration*, Garmisch-Patenkirchen, Germany, 2000, paper I-195.

10 **Schulz, J., Neise, W.** and **Möser, M.** Active noise control in axial turbomachines by flow induced secondary sound sources. 8th AIAA/CEAS Aeroacoustics Conference, Breckenridge, Colorado, 17–19 June 2002, AIAA-2002-2493.

11 **Neuhaus, L.** and **Neise, W.** Active control of aerodynamic and acoustic performance of axial turbomachines. 8th AIAA/CEAS Aeroacoustics Conference, Breckenridge, Colorado, 17–19 June 2002, AIAA-2002-2499.

12 **Neuhaus, L.** and **Neise, W.** Active flow control to improve the aerodynamic and acoustic performance of axial turbomachines. 1st Flow Control Conference, St. Louis, Missouri, 24–27 June 2002, AIAA-2002-2948.

13 **Schulz, J., Fuchs, M., Neise, W.** and **Möser, M.** Active flow control to reduce the tonal noise components of axial turbomachinery. 1st Flow Control Conference, St Louis, Missouri, 24–27 June 2002, AIAA-2002-2949.